THE ASTROPHYSICAL JOURNAL, 553:L189–L191, 2001 June 1

IMAGING POLARIMETRIC OBSERVATIONS OF A NEW CIRCUMSTELLAR DISK SYSTEM

J. R. KUHN, D. POTTER, AND B. PARISE[1]
Institute for Astronomy, University of Hawaii, 2680 Woodlawn Drive, Honolulu, HI 96822
Received 2001 February 22; accepted 2001 April 26; published 2001 May 22

ABSTRACT

Few circumstellar disks have been observed directly. Here we use sensitive differential polarimetric techniques to overcome atmospheric speckle noise in order to image the circumstellar material around HD 169142. The detected envelope or disk is considerably smaller than expectations based on the measured strength of the far-IR excess from this system.

Subject headings: circumstellar matter — techniques: polarimetric

1. INTRODUCTION

Progress toward understanding the evolution of disklike stellar systems will be aided greatly by improved techniques and new imaging measurements of candidate objects. Photometry from the UV to far-IR of several likely unevolved stars show spectral evidence of circumstellar material (see Malfait, Bogaert, & Waelkens 1998). The question as to how these will evolve toward planetary systems is of great interest, but we are far from understanding the general conditions that lead to planet formation from pre–main-sequence objects. With more than 50 planetary systems detected (Marcy & Butler 2000), it is the observational clues to the pre–main-sequence systems that are particularly scarce—only a few resolved observations of circumstellar disk systems exist.

Observing faint circumstellar material environments from ground-based telescopes is typically a feat for adaptive optics (AO), but it is more aptly described as a dynamic range problem, something that is not automatically assured with current AO systems. In particular, we show here how a 4 m telescope at a good site, operating in the *H* band, with only low-order (tip-tilt) wave-front compensation and high dynamic range detectors, can be adequate for extracting smaller than 1% circumstellar signals within an arcsecond of a bright star. The dusty environment of our target (HD 169142) was unsuccessfully searched for earlier (Harvey et al. 1996).

The general problem of extracting a faint optical/IR signal from the scattered light due to atmospheric seeing and telescope diffraction requires a stable point-spread function and a high dynamic range measurement. A high dynamic range can be achieved effectively with coronagraphic observing techniques (assuming a high Strehl ratio is achieved) and using fast-framing IR array detectors, but, unfortunately, from any ground-based optical system, the stability of the point-response function is limited by atmospheric speckle noise. Differential, multiwavelength observations (Racine et al. 1999) have been suggested as a method to minimize such noise, although their approach may be limited by the chromaticity of the residual noise (but see Marois et al. 2000 for a discussion of this technique). Here we demonstrate how differential polarimetric techniques can have significant detection threshold advantages. Mauron & Dole (1998) have achieved excellent detection thresholds using a similar dual-beam polarization technique with nonimaging detectors.

To illustrate this, we consider the problem of detecting the linearly polarized scattered light from a circumstellar disk in the presence of unpolarized scattered light from the central star. We assume a detector that simultaneously images two orthogonal polarization states on distinct regions of the IR camera array. For small scattering angles (less than a few arcseconds), the atmospherically scattered speckle patterns in each polarized brightness component are indistinguishable, so that the difference image constructed from orthogonal polarizations removes the scattered light, leaving a polarized brightness circumstellar image. For real nonphoton counting detectors, the residual noise in the difference image will be limited by calibration flat-fielding uncertainties. These can be minimized with a "double-chop" technique that exchanges the orthogonal polarization illumination on the array at the expense of introducing some speckle noise into the measurement. We describe the post–flat-field residual pixel-to-pixel gain variations in the two images by $[1 + \epsilon_i(\boldsymbol{r})]$, where $i = 1, 2$ and the $\epsilon_i(\boldsymbol{r})$ are two different functions that account for the residual flat-field errors in the two image sections. Using least-squares algorithms described by Kuhn, Lin, & Lorenz (1991), we expect ϵ_i to be of order 10^{-3}.

We take $I(\boldsymbol{r})$ to represent the scattered-light scene in one subimage snapshot and $I'(\boldsymbol{r}) = I(\boldsymbol{r})\,[1 + \delta(\boldsymbol{r})]$ to express the image scene (including speckle changes) in a second snapshot a short time later. Here $\delta(\boldsymbol{r})$ describes the amplitude of the speckle variation from one snapshot to the next. We take $p_{\pm}(\boldsymbol{r})$ as the contribution to the polarized image flux from the circumstellar material. The effect of two polarizers (labeled "+" and "−") is to produce an image scene of scattered (proportional to the input) and circumstellar light, i.e., $K_+ I(\boldsymbol{r})$ and $p_+(\boldsymbol{r})$. The data recorded for the + analyzer at the camera is $d_+ = (1 + \epsilon_1)(K_+ I + p_+)$, and for the − state $d_- = (1 + \epsilon_2)(K_- I + p_-)$. A second snapshot obtained with the + and − polarization images interchanged on the detector yields $d'_+ = (1 + \epsilon_2)(K_+ I' + p_+)$ and $d'_- = (1 + \epsilon_1)(K_- I' + p_-)$. By combining the sum of the differences, we obtain

$$\begin{aligned}[(d_+ - d_-) + (d'_+ - d'_-)]/I(\boldsymbol{r}) &= 2[p_+(\boldsymbol{r}) - p_-(\boldsymbol{r})]/I(\boldsymbol{r}) \\ &+ 2(K_+ - K_-) + [\epsilon_2(\boldsymbol{r}) + \epsilon_1(\boldsymbol{r})](K_+ - K_-) \\ &+ (K_+ - K_-)\delta(\boldsymbol{r}) + [\epsilon_1(\boldsymbol{r}) - \epsilon_2(\boldsymbol{r})][p_+(\boldsymbol{r}) - p_-(\boldsymbol{r})]/I(\boldsymbol{r}).\end{aligned} \tag{1}$$

And we have ignored terms that are as small as the product of ϵ and δ. For most of these observations, the detector read noise is insignificant.

Isolating the circumstellar polarization signal, the first term on the right-hand side of equation (1), is the aim of this analysis.

[1] Ecole Normale Superieure, Department de Physique, 24 Rue Lhomond, 75231 Paris, Cedex 05, France.

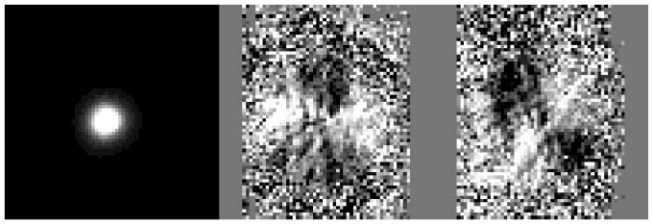

FIG. 1.—Average intensity Stokes Q and U polarization images (normalized as the first term on the right-hand side of eq. [1]). The FWHM of the intensity image is 7 pixels (0.″57). The middle panel shows the vertical polarization, while the right panel displays polarization oriented from upper left to lower right as positive. The full range from dark to light corresponds to $\pm 1.5\%$ polarization. The spatial scale of each image is 5.″2.

All the other terms on the right-hand side of equation (1) describe the effects of flat-fielding and speckle noise. During the observation, we will accumulate temporally interleaved images corresponding to d_+, d_-, d'_+, and d'_-. The polarized flux constants, K_+ and K_-, can be empirically obtained from virtually all of the illuminated pixels by scaling the subimages to minimize their difference. Since there are many pixels, K_+ and K_- can be determined to an accuracy of better than 10^{-4} (significantly better than the photon noise in a single pixel). In this case, it is clear that the noise in the polarization due to flat-fielding errors (the third term on the right-hand side of eq. [1]) can be minimized. By interleaving snapshots and averaging many frames, we can also force $\delta(\boldsymbol{r})$ to be less than 10^{-2} so that the fourth term of equation (1) is also negligible. The double-chopping polarization analysis should eliminate speckle noise from our measurements to the level of 10^{-3} of the background as long as we accumulate at least 10^6 background photons per pixel to overcome photon noise (and read noise) and as long as we can minimize the flat-fielding errors, ϵ. Flat-fielding uncertainties have been the largest concern in applying these techniques.

2. OBSERVATIONS

The United Kingdom Infrared Telescope (UKIRT) and its facility IR polarimeter are well suited for this program. The observations described here were obtained in 2000 September 1–3 with the UKIRT IRCAM InSb camera and the IRPOL polarimeter, which provides simultaneous *e*- and *o*-ray images through a "cold" Wollaston prism. In the H band, the image deviation (and field of view) is about 5″, and the camera scale is 0.″0814 pixel^{-1}. A warm rotating wave plate is mounted ahead of the image plane mask to allow orthogonal polarization states to be interchanged on the detector.

Approximately 10 candidate disk systems from Mannings & Barlow (1998) and Coulson, Walther, & Dent (1998) were selected. Typical H-band observations of these 7–11 mag sources were obtained by co-adding between 10 and 100 0.1–1 s exposure images. The wave plate was rotated by 22.″5 (for a total of four wave-plate angles), and exposures were repeated. The telescope was also offset by as much 0.″3 to three spatially displaced pointings, and the polarization sequence was repeated. Averaged data from the displaced images helped to reduce residual flat-fielding noise. Unpolarized and polarized standard stars from the IRPOL database were also observed.

Several different techniques were used to obtain flat-fielding data. The best calibration was obtained from extended object planetary images. A set of eight displaced Uranus images were obtained for each of the four wave-plate angles. The image displacements ranged up to 1.″5 and were chosen in nonredundant directions in order to apply a least-squares flat-fielding algorithm (Kuhn et al. 1991).

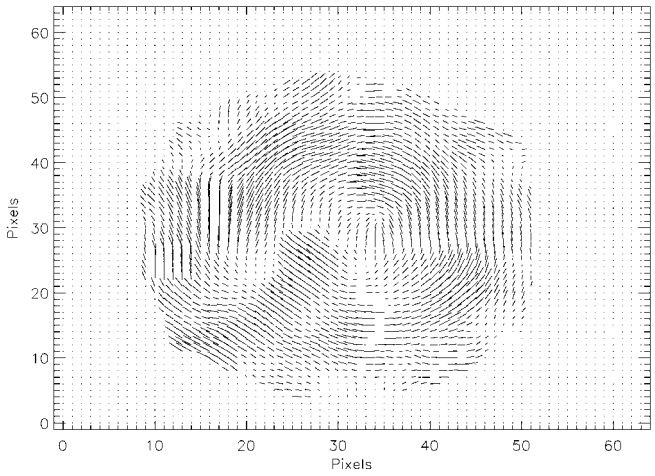

FIG. 2.—Plot of the polarization derived from Q- and U-measurements. The length of the plotted line segments is proportional to the polarization fraction (about 1.5% in the strongest pixels). The Q- and U-data were smoothed with a 5 pixel boxcar average before the plotting and a minimum-intensity threshold defined the pixels to be plotted.

All observations were obtained from similar co-added image sequences using a common IRCAM/IRPOL optical configuration. To define corresponding pixels (scale and offset) in the displaced and polarized subimages, we observed a collection of nearby point sources (the M15 globular cluster). Dark/bias corrections for all frames were derived from equivalent integration time images obtained immediately before each co-added sequence. Separate flat fields were computed and applied for data from each wave-plate angle.

Several program stars are still being analyzed, but one object shows unambiguous evidence of a dusty circumstellar environment with the polarization signature of a face-on disk. HD 169142 (SAO 186777, IRAS 18213−2948) was observed on September 3 at 13:43 UT. A polarization sequence was obtained using 30 2 s exposures. A shorter sequence of 20 0.3 s exposures were also obtained in order to obtain the total stellar flux since longer exposures are saturated in the image core. The seeing during the elapsed 30 minutes of observations was variable but approximately 0.″5 at an air mass of 1.75. This is a bright, $m_B = 8.4$ B9 Ve star at an estimated distance of 145 pc (Sylvester et al. 1996). It has been observed by Yudin, Clarke, & Smith (1999) to be polarimetrically variable over timescales of a day. We are not aware of any spatially resolved observations of this object, although models of its spectral energy distribution (Malfait et al. 1998) suggest that it has two extended circumstellar shells or disks, with the outer one extending from a few tenths to several arcseconds from the star. It should be noted that its conventional identification as a young Herbig Ae/Be star is not ironclad—it shows no evidence of proximity to nebulosity or star-forming regions (G. Herbig 2001, private communication).

3. ANALYSIS AND DISCUSSION

Figure 1 shows the mean intensity and Stokes Q and U polarization images obtained from HD 169142. The Q- and U-images are obtained as in equation (1) by differencing and averaging orthogonal polarization data. The similar but 45°-rotated Q- and U-data show a signature of an optically thin scattering

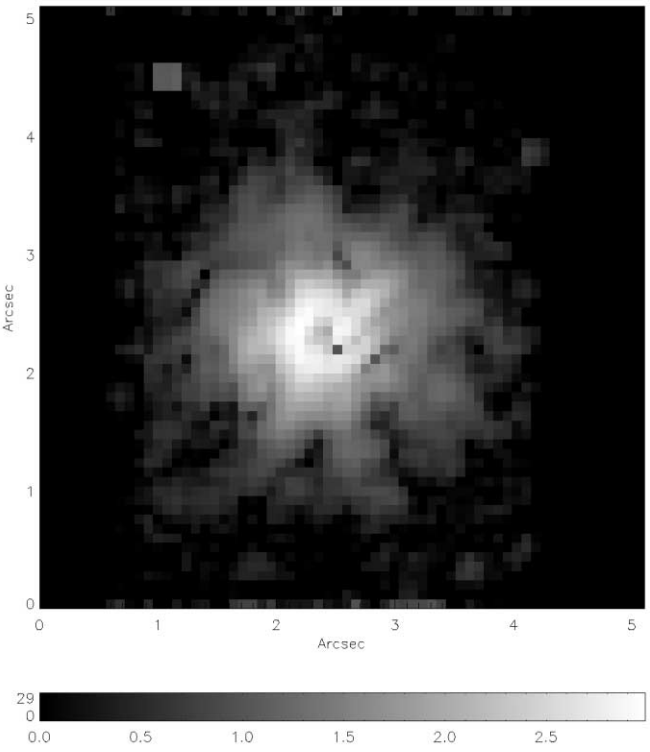

FIG. 3.—Logarithm (base 10) of the polarized brightness. North is to the right, and east is up.

source surrounding the central star. Figure 2 shows how the polarization direction is generally organized in concentric rings around the central source. The total polarized flux is only 7.5×10^{-3} of the total stellar flux. The IR excess–to–stellar luminosity ratio for this system is also small (8.8×10^{-2}; Yudin et al. 1999).

The polarization fraction is not uniform but shows clumpiness over the scale of the image. The polarized brightness in Figure 3 (equal to the polarization fraction times the mean *H*-band surface brightness intensity) provides evidence of scattering inhomogeneity within the circumstellar cloud. The slight elongation of the polarized brightness to the upper right and lower left in Figure 3 is also a robust feature of the HD 169142 circumstellar cloud.

Although the dominant errors in these measurements are from the residual flat-fielding calibration uncertainty, the detected polarization within 1.″7 of the star is highly significant. We estimate the noise from observations of an unpolarized source. Figure 4 plots the ratio of the circularly averaged polarized flux divided by the unpolarized brightness, from HD 169142 and from an unpolarized standard (*dotted curve*). The figure shows the expected polarization fraction bias (Serkowski

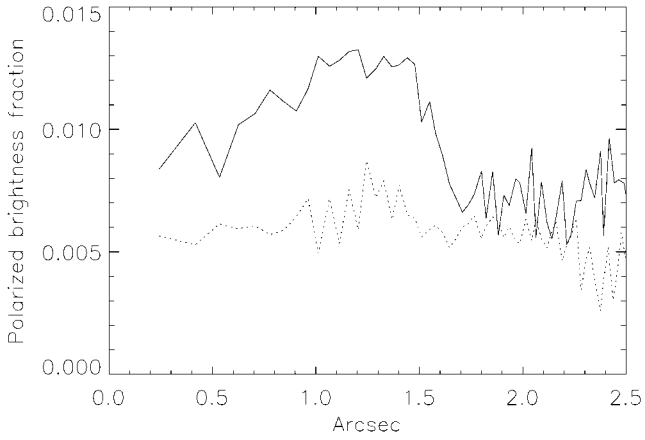

FIG. 4.—Plot of the circular average of the polarized brightness normalized by the mean brightness as a function of distance from the central star. The dotted line shows the noise level from a similar calculation for an unpolarized calibrator star. The circumstellar disk extends to a radius of approximately 1.″5.

1962) of about 0.005 in the standard star observations (*dotted line*). These data have an rms polarization uncertainty of 0.0012. Thus, subject to the assumption that the intrinsic circumstellar material polarization is a weak function of distance from the star, we conclude that the drop in polarized light fraction near 1.″5 is evidence of a disk edge. In any case, the nonzero polarized light fraction measurements within 1.″5 are highly significant, while the light beyond 1.″7 from the source is consistent with unpolarized scattered light from the telescope and atmosphere. Apparently, the disk in HD 169142 has a radius of about 1.″5. In contrast, the thermal model that Malfait et al. (1998) required to describe this system implied a much larger disk size, roughly an order of magnitude bigger than what we observe here.

These observations reveal a faint circumstellar envelope around HD 169142. The relatively small angular extent of this disklike cloud has been measured without high-order adaptive optics. Its detection here demonstrates the utility of dual-beam imaging IR polarimetry for overcoming atmospheric speckle noise and for achieving high photometric dynamic range in the angular vicinity of bright sources.

The United Kingdom Infrared Telescope is operated by the Joint Astronomy Center on behalf of the UK Particle Physics and Astronomy Research Council. We thank the Department of Physical Sciences, University of Hertfordshire, for providing IRPOL2 for the UKIRT. We are indebted to Chris Davis, Sandy Leggett, and the UKIRT staff for their support during these observations. We also acknowledge useful discussions with George Herbig and Ingrid Mann concerning the nature of HD 169142 and its dusty environment.

REFERENCES

Coulson, I. M., Walther, D. M., & Dent, W. R. F. 1998, MNRAS, 296, 934
Harvey, P. M., Smith, B. J., Difrancesco, J., Colome, C., & Low, F. 1996, ApJ, 471, 973
Kuhn, J. R., Lin, H., & Lorenz, D. 1991, PASP, 103, 1097
Malfait, K., Bogaert, E., & Waelkens, C. 1998, A&A, 331, 211
Mannings, V., & Barlow, M. J. 1998, ApJ, 497, 330
Marcy, G., & Butler, R. P. 2000, PASP, 112, 137
Marois, C., Doyon, R., Racine, R., & Nadeau, D. 2000, PASP, 112, 91
Mauron, N., & Dole, H. 1998, A&A, 337, 808
Racine, R., Walker, G., Nadeau, D., Doyon, R., & Marois, C. 1999, PASP, 111, 587
Serkowski, N. 1962, Adv. Astron. Astrophys., 1, 304
Sylvester, R. J., Skinner, C. J., Barlow, M. J., & Mannings, V. 1996, MNRAS, 279, 915
Yudin, R. V., Clarke, D., & Smith, R. A. 1999, A&A, 345, 547